Chromium(III)-Polypyridyls

A Case Study

Nick Serpone
Concordia University, Montreal, Quebec, Canada, H3G 1M8
Morton Z. Hoffman
Boston University, Boston, MA 02215

The photochemistry and photophysics of Cr(III) complexes has had a long and noble history (*1*, *2*). In the preceding paper, Kirk (*3*) has described the behavior of Cr(III)-ammine complexes under UV-visible irradiation. Here, we examine the photochemical and photophysical behavior of chromium(III)-polypyridyl complexes, $Cr(NN)_3^{3+}$, in which NN is 2,2′-bipyridine (bpy) or 1,10-phenanthroline (phen), or one of their substituted derivatives; a comprehensive review was published recently (*4*).

Properties of Ground State $Cr(NN)_3^{3+}$ Complexes

Geometric and Electronic Structure

Although $Cr(NN)_3^{3+}$ possesses dihedral (D_3) symmetry (bidentate NN ligands define the blades of a propeller), it is common to discuss such complexes in terms of octahedral symmetry, O_h, where the ground electronic state is a quartet,[1] $^4A_2$. Cr(III) species possess a d^3 electronic configuration ($t_{2g}^3 e_g^0$ in octahedral microsymmetry); under the influence of a very strong crystal field environment, two electronic transitions are possible: $t_{2g}^3 e_g^0 \rightarrow t_{2g}^2 e_g^1$ and $t_{2g}^3 e_g^0 \rightarrow t_{2g}^1 e_g^2$. At intermediate fields, however, more than two transitions may occur. A typical absorption spectrum of a Cr(III) complex consists of three weak absorption bands (quartet-quartet) in the UV-visible spectral region, and two very weak, spin-forbidden bands (quartet-doublet) in the red range of the visible region. The quartet-quartet bands correspond to the spin-allowed transitions from the $^4A_2$ ground state to the three excited quartet stages $^4T_2$, a^4T_1, and b^4T_1; the two spin-forbidden transitions correspond to $^4A_2 \rightarrow {}^2T_1$ and $^4A_2 \rightarrow {}^2E$. To the extent that these electronic transitions occur between t_{2g} and e_g levels which have predominantly metal character, these states are denoted as metal-centered states and transitions between such states are referred to as metal-centered transitions. These transitions are illustrated in the energy level diagram of Figure 1 for d^3 complexes of octahedral symmetry. In Figure 2 we present the absorption spectra of four typical $Cr(NN)_3^{3+}$ complexes [NN = bpy, phen, 4,4′-Ph_2bpy, 4,7-Ph_2phen].

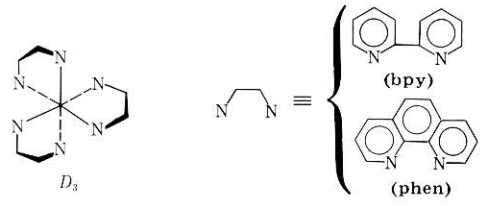

Electronic Absorption Spectra

König and Herzog (*5*) have made a thorough analysis of the ground state absorption spectrum of $Cr(bpy)_3^{3+}$. In octahedral microsymmetry, the three spin-allowed bands at 23.4, 28.9, and 35.6 × 10^3 cm^{-1} arise from the transitions $^4A_2 \rightarrow {}^4T_2$, $^4A_2 \rightarrow a^4T_1$, and $^4A_2 \rightarrow b^4T_1$, respectively. The three unresolved shoulders centered at ~23.4 × 10^3 cm^{-1} originate from vi-

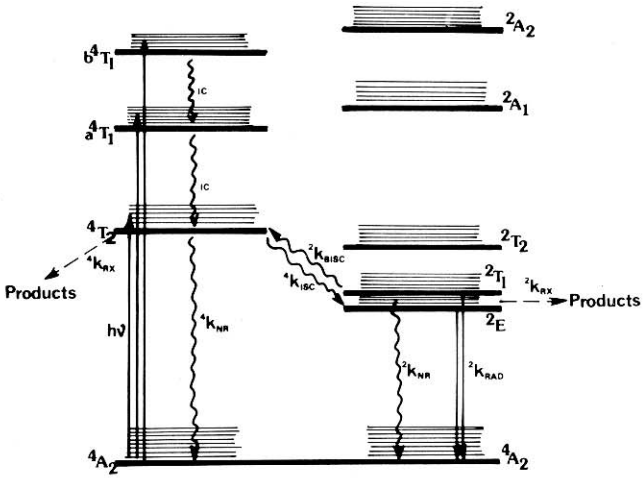

Figure 1. Simplified energy-level diagram of $Cr(NN)_3^{3+}$ complexes; $^4k_{nr}$, $^4k_{isc}$, and $^4k_{rx}$ are the rate constants for the nonradiative, intersystem crossing, and reactive decay modes for the lowest excited quartet state, $^4T_2$; $^2k_{nr}$, $^2k_{bisc}$, and $^2k_{rx}$ are the corresponding rate constants, and $^2k_{rad}$ is the radiative rate constant for the thermally equilibrated ^2E and $^2T_1$ doublet excited states; ic denotes internal conversion. Straight-line arrows refer to radiative transitions, wavy-line arrows refer to nonradiative transitions, and the broken-line arrows depict reactive modes.

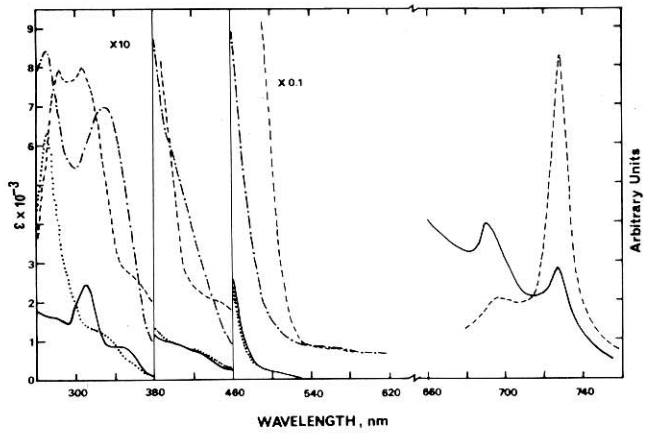

Figure 2. Ground state absorption spectra for four representative $Cr(NN)_3^{3+}$ complexes; (———), $Cr(bpy)_3^{3+}$ in 0.1 *M* HCl aqueous media; (—• —), $Cr(4,4'\text{-}Ph_2bpy)_3^{3+}$ in CH_3OH; (. . .), $Cr(phen)_3^{3+}$ in 0.1 *M* HCl aqueous media; (- - -), $Cr(4,7\text{-}Ph_2phen)_3^{3+}$ in CH_3OH. The two spin-forbidden bands (see text) for $Cr(bpy)_3^{3+}$ (———) are shown on the right, and the spectrum was adapted from reference (*5*); (- - -), luminescence spectrum from $Cr(bpy)_3^{3+}$ in 1.0 *M* HCl aqueous media.

[1] Note that the *g* and *u* subscripts in octahedral symmetry are not used here because the complex lacks a center of symmetry.

Table 1. Properties of $(^4A_2)Cr(NN)_3^{3+}$ and $(^2T_1/^2E)Cr(NN)_3^{3+}$ Complexes [a]

NN	$E°(Cr^{3+}/Cr^{2+})$ (V)	$E°(^*Cr^{3+}/Cr^{2+})$ (V)	$E_{00}(^2E)$ [b] $\times 10^{-3}$ cm^{-1}	$k_q(M^{-1}s^{-1})$ $Fe^{2+} \times 10^{-7}$	$I^- \times 10^{-8}$	$O_2 \times 10^{-7}$	$^2\tau_0$, ms
bpy	−0.26	1.44	13.74	3.7	14	1.7	0.073
4,4′-Me_2bpy	(−0.28)[c]	(1.39)	13.47	2.0	22	17	0.17
4,4′-Ph_2bpy	−0.45	1.25	13.68	0.22	0.40	3.4	0.20
5-Brphen	−0.15	1.55	13.70	8.4	—	3.5	0.18
5-Clphen	−0.17	1.53	13.74	12	80	3.7	0.18
5-Phphen	−0.21	1.49	13.70	4.5	—	5.5	0.22
4,7-Ph_2phen	(−0.26)[c]	(1.41)	13.46	2.5	59	31.0	0.57
phen	−0.28	1.42	13.74	3.2	21	2.7	0.33
5,6-Me_2phen	−0.29	1.40	13.66	2.6	—	8.5	0.42
5-Mephen	−0.30	1.39	13.70	3.4	—	5.7	0.42
4,7-Me_2phen	−0.45	1.23	13.62	0.60	1.5	19.0	0.57
3,4,7,8-Me_4phen	(−0.57)[c]	(1.11)	13.57	0.092	0.47	15.0	0.64

[a] For experimental details and conditions, see reference (*4*).
[b] Taken from reference (*44*).
[c] Estimated by interpolation from a Marcus log k_q versus log K_{12} plot; see reference (*26*).

brational co-excitation involving coupling of electronic *d-d* transitions and vibrational transitions within the bpy ligand. Such coupling implies some electron delocalization within the excited states (i.e., some degree of π bonding). The bands at 32.7 and 42.1 $\times 10^3$ cm^{-1} are due to bpy ligand-centered transitions, $^1A_1 \rightarrow {}^1B_1$ and $^1A_1 \rightarrow {}^1A_1$, respectively (*5*). The lowest-energy multicomponent band arises from the $^4A_2 \rightarrow {}^4T_2$ transition and this band yields the ligand field parameter Δ. For substituted $Cr(NN)_3^{3+}$, the spectral profile is dependent on the nature of the ligand substituents (*6*). Both methyl and phenyl substitution at the 4,4′-positions of the bpy ligand cause a slight blue shift in the bands corresponding to the $^4A_2 \rightarrow {}^4T_2$ transition. By contrast, methyl substitution on the phen ligand framework blue-shifts this low-energy transition, while phenyl- and halo-substitution cause a red shift. In addition, phenyl substitution on both bpy and phen ligands significantly increase the molar absorptivity.

Redox Potentials

Formal redox potentials for the couples $Cr(NN)_3^{3+}/Cr(NN)_3^{2+}$ are summarized in Table 1. In all cases, the $Cr(NN)_3^{2+}$ species are moderately good reducing agents with substituents dramatically affecting their reducing character. For both bpy and phen complexes, electron-donating methyl substituents increase the reducing ability of $Cr(NN)_3^{2+}$, whereas electron-withdrawing halo and phenyl substituents decrease the reducing ability. Also noteworthy are the positions of the substituents in this regard. Methyl substitution at the 5,6-positions of the phen framework hardly affects $E°[Cr(NN)_3^{3+}/Cr(NN)_3^{2+}]$ compared to the parent phen complex, but substitution at the 4,7-positions significantly decreases $E°[Cr(NN)_3^{3+}/Cr(NN)_3^{2+}]$ by ~0.2 V. This suggests that in the latter case, electron density is shifted to the Cr—N bond.

Thermal Reactivity

Knowledge of structure-reactivity relationships of ground state $(^4A_2)Cr(NN)_3^{3+}$ complexes is important in the understanding and elucidation of the photoreactivity of these complexes. $Cr(bpy)_3^{3+}$thermally aquates (reaction (1)) in the pH range 0–10.7 via pH-dependent (see Fig. 3), first order kinetics with $k_{th} < 10^{-8}s^{-1}$ at pH ≤ 6, and $4.7 \times 10^{-7}s^{-1}$ at pH 9–10.7 and 11°C (*7*).

$$Cr(NN)_3^{3+} \xrightarrow[k_{th}]{H^+/H_2O} Cr(NN)_2(H_2O)_2^{3+} + NNH^+ \quad (1)$$
$$\xrightarrow[k_{th}]{OH^-/H_2O} Cr(NN)_2(OH)_2^+ + NN$$

Aquation appears to proceed via an interchange mechanism involving, as the rate determing step, formation of a

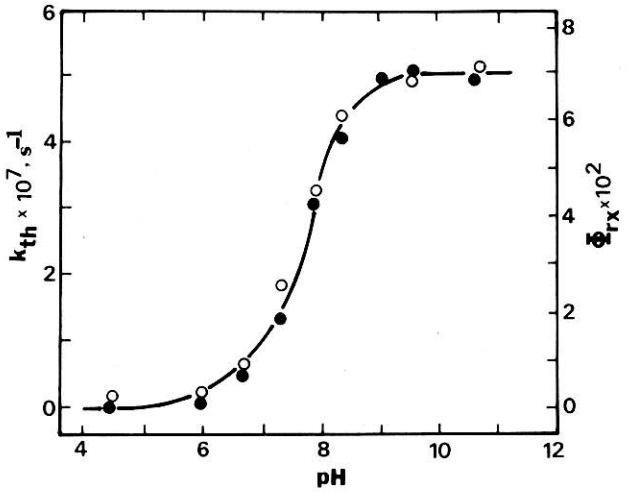

Figure 3. Dependence of k_{th} for the thermal aquation reaction (●) on pH, 11°C, ionic strength 1.0 *M* with NaCl; from reference (*7*). For comparison, the dependence of the quantum yield (Φ_{rx}) of the photochemical reaction (O) on pH is also indicated; 11°C, ionic strength 1.0 *M* with NaCl, air-equilibrated solutions; adapted from reference (*8*).

$Cr(NN)_3(H_2O)^{3+}$ intermediate by nucleophilic attack of a water molecule at the Cr(III) center. The very small and pH-independent k_{th} at pH ≤ 6 can be rationalized in terms of relaxation of the initially-formed intermediates back to $Cr(NN)_3^{3+}$ via acid-dependent and -independent pathways (reaction (2)) (*8*).

$$Cr(NN)_3^{3+} + H_2O \underset{H^+}{\rightleftharpoons} Cr(NN)_3(H_2O)^{3+} \quad (2)$$

Subsequently, $Cr(NN)_3(H_2O)^{3+}$ can undergo deprotonation to form the short-lived $Cr(NN)_3(OH)^{2+}$ species as shown by the inflection point at pH 6–9 in the plot of k_{th} versus pH illustrated in Figure 3. This hydroxy intermediate can then undergo irreversible loss of monodentate NN.

$$Cr(NN)_3(OH)^{2+} \xrightarrow[OH^-]{} Cr(NN)_2(OH)_2^+ + NN \quad (3)$$

The plateau region at pH 9–10.7 reflects the complete titration of $Cr(NN)_3(H_2O)^{3+}$ so that k_{th} represents the rate constant for the rate-determining attack of H_2O on $Cr(NN)_3^{3+}$. The thermal substitution reaction has been extended to include the pH range 10.7–14 for $Cr(bpy)_3^{3+}$ (*9*) and the pH range 0–14 for $Cr(phen)_3^{3+}$ (*10*). The thermal behavior of the latter complex parallels identically that of $Cr(bpy)_3^{3+}$. Above pH 10.7, k_{th} is linearly dependent on $[OH^-]$ in the range 10.7 ≤ pH ≤ 12.2, indicating possible OH^- attack of the chromium(III) core. Where $[OH^-] = 0.1–1.0\ M$, k_{th} varies as $[OH^-]^2$; ion pairs

Table 2. Thermal Activation Parameters for $Cr(bpy)_3^{3+}$ and $Cr(phen)_3^{3+}$ [a]

Activation Parameter	pH ~ 10		pH ~ 12		0.50 M OH^-	
	bpy	phen	bpy	phen	bpy	phen
$\Delta H^{\ddagger}_{298}$, kcal/mol	22.3	23.3	20.7	21.6	18.9	20.8
$\Delta S^{\ddagger}_{298}$, eu	−8.8	−8.4	−12.6	−11	−11	−5
k_{298}, s^{-1}	3.3×10^{-6}	7.9×10^{-7}	6.9×10^{-6}	4.3×10^{-6}	2.9×10^{-4}	1.9×10^{-4}

[a] From references (*7*, *9*, *10*); in 0.008 *M* Britton-Robinson buffer; ionic strength = 1.0 *M* with NaCl.

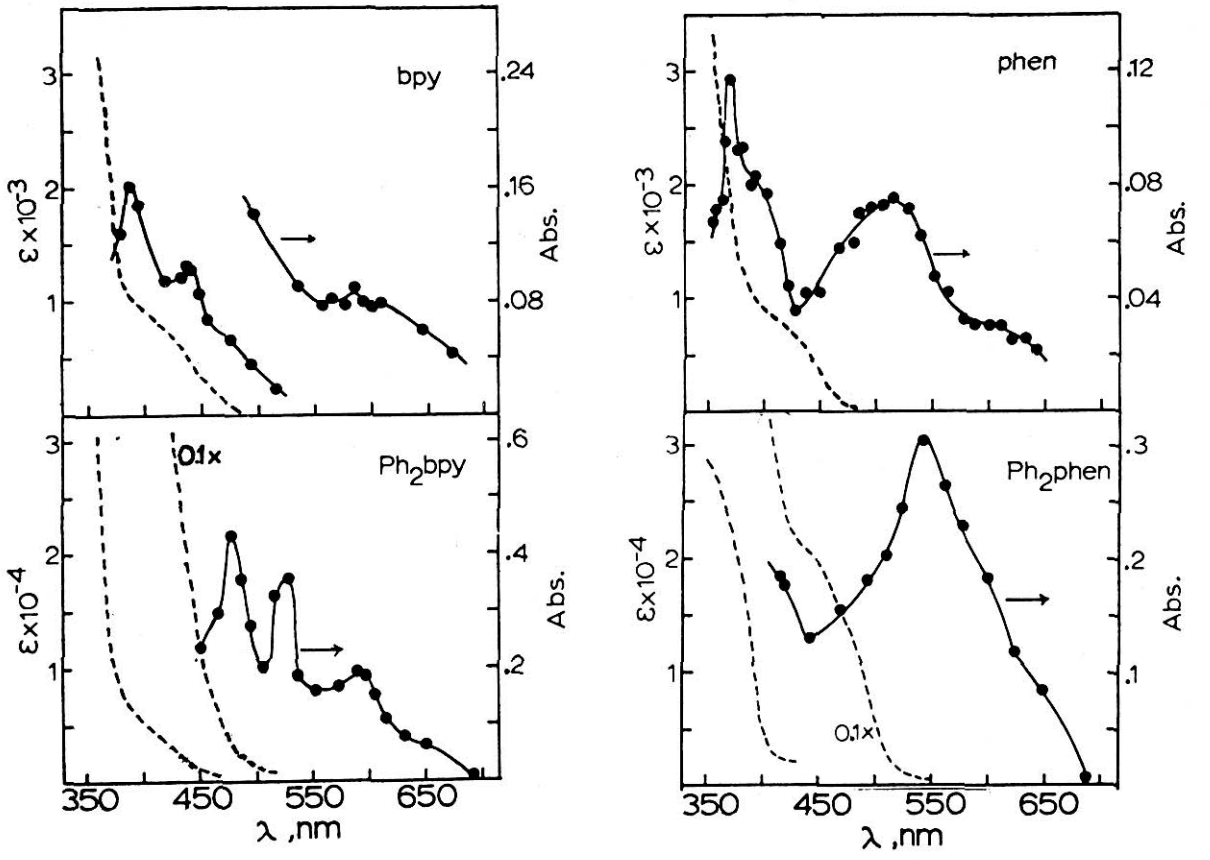

Figure 4. Absorption spectra (●—●) of the transient species $(^2E)Cr(NN)_3^{3+}$ obtained by flash photolysis absorption techniques in N_2-purged acidic media (1 *M* HCl) at 22°C; concentration of complex ~10^{-5} *M*; spectra were measured 40 μs after the flash except for the bpy and phen complexes for which spectra were taken 150 μs after the flash; (- - -), corresponding $^4A_2$ ground state spectra. Break in the $Cr(bpy)_3^{3+}$ transient spectrum results from a change in concentration used for $Cr(bpy)_3^{3+}$. *Adapted from reference (6).*

appear to be implicated in the formation of $Cr(NN)_3(OH)^{2+}$ species. The rate constants and activation parameters for the thermal aquation of $Cr(bpy)_3^{3+}$ and $Cr(phen)_3^{3+}$, under identical experimental conditions, are given in Table 2; the similarity in the activation parameters supports a common mechanism for the two complexes.

Properties of Excited $(^2T_1/^2E)Cr(NN)_3^{3+}$ Complexes

Energetics and Structure

Absorption of light into the lowest energy quartet ligand field band of a Cr(III) complex populates a vibrationally excited Franck-Condon quartet state (isogeometric with the ground state) which subsequently relaxes to the thermally-equilibrated (*thexi*) (*11*) quartet state ($^4T_2^0$). This *thexi* state must be severely distorted with respect to the $^4A_2$ ground state inasmuch as the promotion of an electron from a predominantly nonbonding $d\pi$ orbital (d_{xy}, d_{yz}, and d_{xz}) to a formally σ^* antibonding orbital (d_{z^2} or $d_{x^2-y^2}$) must result in increased Cr—N bond lengths. Any fluorescence ($^4T_2 \rightarrow {}^4A_2$) is expected to be broad and red-shifted with respect to the corresponding absorption band ($^4A_2 \rightarrow {}^4T_2$). However, no such fluorescence emission has been observed in $Cr(NN)_3^{3+}$ complexes in fluid solutions at room temperature or in low temperature glasses and so decay of the quartet state via this path is inconsequential. The energy of $^4T_2^0$ is unknown but has been estimated to be at ~59–62 kcal above the ground state (*8*).

As depicted in Figure 1, the quartet state can dissipate its excess energy via nonradiative decay to $^4A_2(^4k_{nr})$, via nonradiative decay (intersystem crossing) to the spin-forbidden states $^2T_1/^2E(^4k_{isc})$, and via reactive decay ($^4k_{rx}$) to give products. These lowest energy doublet states are not expected to be distorted with respect to $^4A_2$ inasmuch as the $^4A_2 \rightarrow {}^2T_1/^2E$ transition involves no electron promotion to σ^* antibonding orbitals; rather, electron spin-pairing or spin-flip occurs within the t_{2g} level, i.e., the transition is intraconfigurational. Cr—N bond lengths are, therefore, expected to be nearly identical for $^4A_2$ and $^2T_1/^2E$. Indeed, the nuclear equilibrium geometries of $^4A_2$ and $^2T_1/^2E$ are essentially identical inasmuch as absorption ($^4A_2 \rightarrow {}^2T_1/^2E$) and emission ($^2T_1/^2E \rightarrow {}^4A_2$) maxima are coincident, there being no Stokes shift (*12*) (see Fig. 2). The 0-0 doublet levels occur at ~39 kcal above the ground state (Table 1).

Emission and Absorption Spectra

The emission spectral bands, which represent the 0-0 transitions of the $^2T_1/^2E \rightarrow {}^4A_2$ electronic transitions, are only slightly sensitive to the nature of the ligand substituents. Table 1 reveals that substitution varies the energy of the low energy transitions in the order: bpy > 4,4′-Me_2bpy > 4,4′-Ph_2bpy. Ligand substitution on the phen complexes decreases the energy of the ^2E state in the order: phen ~ 5-Clphen > 5-Brphen ~ 5-Phphen ~ 5-Mephen > 5,6-Me_2phen > 4,7-Me_2phen > 3,4,7,8-Me_4phen > 4,7-Ph_2phen.

The doublet state absorption spectra of $Cr(NN)_3^{3+}$ complexes have been obtained by conventional microsecond flash photolysis techniques (*6*); those for which NN = bpy, 4,4′-Ph_2bpy, phen, and 4,7-Ph_2phen are illustrated in Figure 4. Where NN = bpy, the spectrum shows bands at 590, 445, and 390 nm with shoulders at ~650 and 475 nm (*8*). The entire spectrum decays via first-order kinetics in acidic, neutral, and alkaline media with $k = 1.6 \times 10^4 s^{-1}$ at 22°C. The transient absorption is quenched by oxgyen ($1.7 \times 10^7 M^{-1}s^{-1}$) (*8*), I^- ($1.2 \times 10^9 M^{-1}s^{-1}$) and Fe^{2+}_{aq} ($\sim 10^8 M^{-1}s^{-1}$) (*13*). Coincidence of the decay of the phosphorescence emission ($^2E \rightarrow {}^4A_2$) and decay of the transient absorption identified this transient as the ^2E state; this was further substantiated by similar temperature dependencies exhibited by the transient and phosphorescence decays, as well as by the similarities evident in the oxygen and iodide ion quenching results (Table 1). Phenyl substitution at the 4,4′-positions of $Cr(bpy)_3^{3+}$ red-shifts both the 390- and 445-nm bands of $(^2E)Cr(bpy)_3^{3+}$ to 480 and 525 nm, respectively. The band at 590 nm is not sensitive to ligand substituents. This indicates that the doublet manifold reached by absorption is predominantly metal-centered. The remaining two higher energy bands, red-shifted by the presence of substituents, must correspond to electronic transitions to doublet states containing some ligand character and are probably $^2E \rightarrow {}^2$(LMCT) transitions. The doublet absorption spectrum of $*Cr(phen)_3^{3+}$ is characterized by a broad band centered at ~515 nm and appears sensitive to phenyl substitution.

Excited State Lifetimes

The lifetimes of the $^2T_1$ and ^2E states (*14*) responsible for the two emission bands from excited $Cr(bpy)_3^{3+}$ are identical indicating that these two states are in thermal equilibrium and are often denoted simply as ^2E. The observed lifetime of ^2E, $^2\tau_{obs} = 1/\Sigma^2 k$, where ^2k represents the rate constant of the individual decay modes. In the absence of quenchers and other environmental perturbations, $^2\tau_{obs} = 1/(^2k_{nr} + {}^2k_{rx} + {}^2k_{rad} + {}^2k_{bisc})$. The ^2E states of $Cr(NN)_3^{3+}$ react with water ($^2k_{rx}$) in competition with radiative ($^2k_{rad}$) and nonradiative ($^2k_{nr}$) decay back to $^4A_2$ species; back intersystem crossing ($^2k_{bisc}$) to $^4T_2$ appears to be unimportant (*15*). For $Cr(bpy)_3^{3+}$, radiative decay is insignificant ($^2\Phi_{rad} \sim 10^{-3}$) (*6*, *16*) in comparison with nonradiative ($^2\Phi_{nr} \sim 0.9$) and reactive ($^2\Phi_{rx} \sim 0.1$) decay modes. Thus, $^2\tau_{obs} \sim 1/(^2k_{nr} + {}^2k_{rx})$, with the nonradiative decay mode being the predominant decay channel of ^2E (*17*). By contrast, chemical reaction is the important decay mode of the ^2E state of *trans*-$Cr(NH_3)_2(NCS)_4^-$ (*18*). Under high laser power, $(^2E)Cr(phen)_3^{3+}$ and $(^2E)Cr(4,7\text{-}Me_2phen)_3^{3+}$ decay via a second-order, doublet-doublet annihilation process (*19*).

Interaction with Solution Medium

The value of $^2\tau_{obs}$ is strongly dependent on solution medium. The lifetime of ^2E is prolonged by the presence of anions. At $[ClO_4^-] > 1\ M$ in aqueous solution, $^2\tau_{obs}$ and $^2\Phi_{rad}$ are markedly increased and the quantum yield of photoaquation ($^2\Phi_{rx}$) is decreased for both $Cr(bpy)_3^{3+}$ and $Cr(phen)_3^{3+}$ (*20*). This anion effect is the result of changes in the nonradiative and reactive rate constants with the latter exhibiting a greater decrease (*17*). Such ^2E-lifetime prolongation effected by high concentrations of anions appears to be a general phenomenon

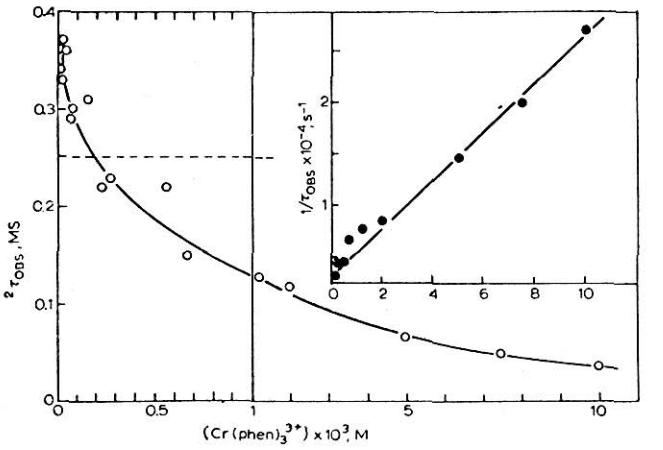

Figure 5. Lifetime of $(^2E)Cr(phen)_3^{3+}$ as a function of [substrate] in deaerated aqueous solutions at 22°C, (O), 1.0 *M* HCl; (- - -), deaerated neat water. Insert represents a plot of $1/^2\tau_{obs}$ for $Cr(phen)_3^{3+}$ as a function of [substrate] in deaerated 1.0 *M* HCl solution at 22°C. From reference (*3*).

in $Cr(NN)_3^{3+}$ complexes (*6*, *21*, *22*). In the case of ClO_4^-, extensive ion pairing occurs between the Cr(III) core and the anions in the interligand pockets as well as in the solvation sphere, thereby curbing access to the core by solvent water molecules resulting in a decrease of $^2k_{rx}$; also, the "wedged" anions in the pockets can reduce the motion of the critical vibrational modes in the ligand. These effects are more pronounced in the $Cr(bpy)_3^{3+}$ complex with the more rigid phen analogue being less prone to such anion perturbations; in 11.7 *M* $HClO_4$, $^2\tau_{obs}$ for $(^2E)Cr(bpy)_3^{3+}$ has been increased by a factor of ~10, but only by a factor of ~2 for $(^2E)Cr(phen)_3^{3+}$ relative to $^2\tau_{obs}$ in 1 *M* Cl^- media (*20*).

Furthermore, $^2\tau_{obs}$ is increased with decreasing [substrate] in Cl^- aqueous media. For $Cr(phen)_3^{3+}$ in 1 *M* HCl at 22°C, $^2\tau_{obs}$ is increased by an order of magnitude (0.038 ms to 0.33 ms) as [substrate] is decreased from 1×10^{-2} *M* to 1×10^{-5} *M*; this effect is illustrated in Figure 5. Similar results are obtained in 1 *M* NaCl indicating that the effect is mediated by the Cl^- anions; no effect is observed in the absence of anions. By comparison, to observe the effect in $Cr(bpy)_3^{3+}$ requires 5 *M* HCl. The observed lifetime variation of Figure 5 follows good quenching kinetics; $^2k_{obs} = {}^2k_0 + {}^2k_g[Cr(NN)_3^{3+}]$, where $^2k_0 (= 1/^2\tau_0)$ is the first-order rate constant for deactivation of ^2E at infinite substrate dilution and ^2k_g is the second-order rate constant for the quenching of ^2E by the ground state complex (reaction (4)).

$$(^2E)Cr(NN)_3^{3+} + (^4A_2)Cr(NN)_3^{3+} \xrightarrow[Cl^-]{^2k_{obs}} 2(^4A_2)Cr(NN)_3^{3+} \quad (4)$$

Thus, for $Cr(phen)_3^{3+}$ in 1 *M* HCl media at 22°C, $^2k_0 = 3.0 \times 10^3 s^{-1}$ and $^2k_g = 2.3 \times 10^6 M^{-1}s^{-1}$, while $^2k_0 = 1.0 \times 10^4 s^{-1}$ and $^2k_g = 1.3 \times 10^6 M^{-1}s^{-1}$ for $Cr(bpy)_3^{3+}$ in 5 *M* HCl media at 22°C (*22*). The other $Cr(NN)_3^{3+}$ complexes show similar behavior (*21*) with the data demonstrating that, in addition to the solution medium, both the size of the Cr(III) cation and the nature of the ligand substituents have an effect on ^2k_g. This second-order rate constant reflects the encounter of ion-paired ground state $[(^4A_2)Cr(NN)_3^{3+} \cdots Cl^-]$ and excited state $[(^2E)Cr(NN)_3^{3+} \cdots Cl^-]$ species which can be viewed as forming an "ion-bridged excimer," $*[Cr(NN)_3^{3+} \cdots Cl^- \cdots Cr(NN)_3^{3+}]$, which rapidly decays nonradiatively via coupling of the vibrational modes in the aggregate. Ground state quenching of Cr(III) excited states in solid matrices has previously been attributed to formation of such aggregates (*23*). The generality of ground state quenching for $Cr(phen)_3^{3+}$ in other anionic media has recently been demonstrated (*24*).

Clearly $^2\tau_{obs}$ must be established for the specific experimental conditions; $^2\tau_0$ reflects the nonradiative and reactive

decay modes. As evident in Table 1, subtle modification of the polypyridyl ligand by the variation of substituents alters $^2\tau_0$. We see that 4,4′-substitution on the bpy framework and 4,7-dimethyl, 4,7-diphenyl, 5-methyl, 5,6-dimethyl, and 3,4,7,8-tetramethyl substitution on the phen ligand increases $^2\tau_0$, while 5-bromo, 5-chloro, and 5-phenyl substitution on phen decreases $^2\tau_0$; it appears that the greater vibrational rigidity of the phenanthroline complexes decreases the nonradiative decay mode relative to the analogous bipyridyl complexes, with consequentially larger values of $^2\tau_0$. These variations in the doublet lifetimes are understood in terms of the ligand acting as both an oscillating perturbation dipole and as an energy acceptor. Halo substituents could provide an increased dipole perturbation that would increase $^2k_{nr}$; by comparison, methyl and phenyl substitution on the polypyridine could decrease the perturbation dipole, probably through their effect on the critical ligand vibrational modes. Moreover, the large interligand pockets in the dihedral $Cr(NN)_3^{3+}$ structure could allow solvent molecules to penetrate close to the Cr(III) core and provide an additional decay channel; substituents on the ligands that can isolate the metal core from solvent molecules should lead to increased $^2\tau_0$ (*6*). This structural effect is most evident at the 4,7-positions in the phen ligand framework. Variations of solvent medium also affects $^2\tau_{obs}$; Van Houten and Porter (*25*) found $^2\tau_{obs} \sim 3\mu s$ for $Cr(bpy)_3^{3+}$ in dimethylformamide.

Redox Potentials

Transition metal polypyridyl complexes have proven of value in electron- and energy-transfer studies inasmuch as they provide a wide range of excited state properties that can be "fine tuned" by alteration of the metal center, by alteration of the type of ligand, or simply by variation of the substituents on the polypyridine framework. One property of excited states that is dependent on ligand substituents is the redox potential; the changes are expected to parallel those noted earlier for the ground state species.

Where the Stokes shift between ground state absorption and excited state emission is small, and the differences in shape, size, and solvation between the two states are also small, the entropy differences between ground and excited states are negligible. The redox potentials for the $(^2E)Cr(NN)_3^{3+}$ species can be estimated from eqn. (5), where $E_{00}(*Cr^{3+}/Cr^{3+})$ is the one electron potential corresponding to the 0-0 spectroscopic energy of the excited state (~1.7 eV).

$$E°(*Cr^{3+}/Cr^{2+}) = E°(Cr^{3+}/Cr^{2+}) + E_{00}(*Cr^{3+}/Cr^{3+}) \quad (5)$$

The redox potentials evaluated in this manner are given in Table 1 (*6*, *26–28*). The validity of this procedure for $Cr(NN)_3^{3+}$ complexes has been verified by Balzani and coworkers (*29*). The ^2E complexes are moderately strong oxidizing agents compared to the $^4A_2$ species; this effect is a consequence of the excitation of an electron from a low energy orbital to a higher energy orbital leading to a reduction of the ionization potential and to an increase of the electron affinity. The 5-halo phen complexes are the strongest oxidants while the poorest oxidizing agents are those containing methyl-substituted phen ligands.

Electron and Energy Transfer Reactions

Of the various decay paths available to excited states, the principal quenching modes are electron transfer and energy transfer. It is often difficult to discriminate between these two quenching modes inasmuch as energy-transfer reactions can lead to the same oxidized or reduced products expected from electron-transfer reactions, and electron-transfer reactions may yield, in the end, nonreduced or nonoxidized products (*30*). Knowledge of the energy of the ^2E excited state, the energy of the lowest excited state of the quencher, and the ground state redox potentials of $Cr(NN)_3^{3+}$ has been useful in assigning the operative quenching mode. Correlations between the quenching rate constants, ^2k_q, and the thermodynamic quantities involved have also been critical, in some cases, in defining the nature of the quenching mechanism.

Experiments have been carried out (*13*) to show that the emission of $(^2E)Cr(bpy)_3^{3+}$ is quenched by $Ru(bpy)_3^{2+}$ via reductive electron transfer. Energy transfer is not possible inasmuch as the energies of the lowest excited states of $Cr(bpy)_3^{3+}$ and $Ru(bpy)_3^{2+}$ are 13.7×10^3 and 17.1×10^3 cm^{-1}, respectively. For electron transfer, the redox potentials for the $*Cr(bpy)_3^{3+}/Cr(bpy)_3^{2+}$ and $Ru(bpy)_3^{3+}/Ru(bpy)_3^{2+}$ couples are 1.44 V and 1.30 V versus NHE (*31*), respectively. Flash photolysis experiments demonstrate that $(^2E)Cr(bpy)_3^{3+}$ is quenched by I^- and $Ru(bpy)_3^{2+}$ via electron transfer reactions (6)–(8); reaction (9) constitutes back electron transfer of the charge-separated species.

$$Cr(bpy)_3^{3+} \xrightarrow{h\nu} (^4T_2)Cr(bpy)_3^{3+} \rightarrow (^2E)Cr(bpy)_3^{3+} \quad (6)$$

$$(^2E)Cr(bpy)_3^{3+} + I^- \rightarrow Cr(bpy)_3^{2+} + I \quad (7)$$

$$(^2E)Cr(bpy)_3^{3+} + Ru(bpy)_3^{2+} \rightarrow Cr(bpy)_3^{2+} + Ru(bpy)_3^{3+} \quad (8)$$

$$Ru(bpy)_3^{3+} + Cr(bpy)_3^{2+} \rightarrow Ru(bpy)_3^{2+} + Cr(bpy)_3^{3+} \quad (9)$$

The rate constants of reactions (7)–(9) are 1.4×10^9 (*6*), 4.0×10^8 (*32*) and 2.6×10^9 (*13*) $M^{-1}s^{-1}$, respectively. The products of reaction (7) are not observed because the geminate products undergo prompt back electron transfer within the solvent cage; however, in the absence of I^-, the electron transfer products of reaction (8) are observed. Because $Cr(bpy)_3^{3+}$ can quench the lowest excited state of $Ru(bpy)_3^{2+}$, reactions (10) and (11) also occur

$$Ru(bpy)_3^{2+} \xrightarrow{h\nu} {}^1(MLCT)Ru(bpy)_3^{2+} \rightarrow {}^3(MLCT)Ru(bpy)_3^{2+} \quad (10)$$

$${}^3(MLCT)Ru(bpy)_3^{2+} + Cr(bpy)_3^{3+} \rightarrow Ru(bpy)_3^{3+} + Cr(bpy)_3^{2+} \quad (11)$$

$k_{11} = 3.3 \times 10^9$ $M^{-1}s^{-1}$ (*32*). $(^2E)Cr(bpy)_3^{3+}$ is quenched by aliphatic and aromatic amines and methoxybenzenes via reductive electron transfer leading to one-electron oxidized products of the quenchers (*29*). Luminescence quenching of $(^2E)Cr(bpy)_3^{3+}$ by various transition metal cyano complexes has shown that reductive electron transfer occurs with $Mo(CN)_8^{4-}$, $Fe(CN)_6^{4-}$, $Ru(CN)_6^{4-}$, and $Ni(CN)_4^{2-}$ and oxidative electron transfer with $Fe(CN)_6^{3-}$ and $Co(CN)_6^{3-}$; with $Cr(CN)_6^{3-}$ quenching occurs via energy transfer (*33*). The relationship between k_q and the redox potentials of the excited states and quencher species is consistent with reductive or oxidative electron transfer. Plots of log k_q versus the driving force for electron transfer, ΔG_e°, show no inverted region as predicted by the Marcus theory of electron transfer (*34*). There is no decrease in k_q at the larger negative values of ΔG_e° (*29*, *33*); rather, the trend in k_q follows the modified theory of Rehm and Weller (*35*).

As Table 1 shows, I^- quenches the ^2E states of all 12 $Cr(NN)_3^{3+}$ complexes and the values of k_q range over two orders of magnitude. To the extent that the lowest excited states of I^- have energies greater than 37.0×10^3 cm^{-1}, an energy transfer pathway is ruled out. The k_q values decrease as the oxidizing ability of the $(^2E)Cr(NN)_3^{3+}$ species decreases; the strongest oxidant, $(^2E)Cr(5\text{-}Clphen)_3^{3+}$, has the highest k_q while the weakest oxidant, $(^2E)Cr(3,4,7,8\text{-}Me_4phen)_3^{3+}$, has the lowest value of k_q. For quenching of $(^2E)Cr(NN)_3^{3+}$ by Fe_{aq}^{2+}, the formation of $Cr(NN)_3^{2+}$ and its subsequent second-order reaction with Fe_{aq}^{3+} is observed (*6*). The availability of low-lying states of Fe_{aq}^{2+} at 10.4×10^3 cm^{-1} ($^5T_{2g}$) and at ~14.4 $\times 10^3$ cm^{-1} (probably $^3T_{1g}$) (*36*) above the $^1A_{1g}$ ground state renders direct energy transfer energetically feasible. A scheme for $(^2E)Cr(NN)_3^{3+}$-Fe_{aq}^{2+} quenching involving both electron- and energy-transfer modes is depicted by reactions (12)–(17), where {|} denotes an encounter pair in a solvent cage with reaction (14) thermodynamically allowed.

$$(^2E)\mathrm{Cr(NN)_3^{3+}} + \mathrm{Fe_{aq}^{2+}} \rightarrow \mathrm{Cr(NN)_3^{3+}} + {}^*\mathrm{Fe_{aq}^{2+}} \quad (12)$$

$$\mathrm{Cr(NN)_3^{3+}} + {}^*\mathrm{Fe_{aq}^{2+}} \rightleftharpoons \{\mathrm{Cr(NN)_3^{3+}}|{}^*\mathrm{Fe^{2+}}\} \quad (13)$$

$$\{\mathrm{Cr(NN)_3^{3+}}|{}^*\mathrm{Fe^{2+}}\} \rightarrow \{\mathrm{Cr(NN)_3^{2+}}|\mathrm{Fe^{3+}}\} \quad (14)$$

$$(^2E)\mathrm{Cr(NN)_3^{3+}} + \mathrm{Fe_{aq}^{2+}} \rightarrow \{(^2E)\mathrm{Cr(NN)_3^{3+}}|\mathrm{Fe^{2+}}\} \quad (15)$$

$$\{(^2E)\mathrm{Cr(NN)_3^{3+}}|\mathrm{Fe^{2+}}\} \rightarrow \{\mathrm{Cr(NN)_3^{2+}}|\mathrm{Fe^{3+}}\} \quad (16)$$

$$\{\mathrm{Cr(NN)_3^{2+}}|\mathrm{Fe^{3+}}\} \rightarrow \mathrm{Cr(NN)_3^{2+}} + \mathrm{Fe_{aq}^{3+}} \quad (17)$$

For the energy-transfer route to be of any consequence, $k_{14} > k_{16}$. Energy transfer appears to be inconsequential in the quenching of $(^2E)\mathrm{Cr(NN)_3^{3+}}$ by $\mathrm{Fe_{aq}^{2+}}$ inasmuch as the reorganization energy in the electron-transfer step (14) is expected to be much larger than that of reaction (16) because electron transfer originates from an antibonding e_g level in step (15); in reaction (16), a t_{2g} electron is involved. Moreover, the orbitals implicated in reaction (16) have identical t_{2g} symmetry while in reaction (14) the donor orbital is e_g and the acceptor orbital is t_{2g}. The variations in k_q (Table 1) support direct electron transfer with the stronger oxidants; the 5-halo phen complexes give the largest rates. An additional benefit in obtaining k_q from electron-transfer processes is the estimation of the self-exchange rate for reaction (18); $k_{18} \sim 10^8$–$10^9 \mathrm{M^{-1}s^{-1}}$ (*26*, *27*).

$$(^2E)\mathrm{Cr(NN)_3^{3+}} + \mathbf{Cr}\mathrm{(NN)_3^{2+}} \rightarrow \mathrm{Cr(NN)_3^{2+}} + (^2E)\mathbf{Cr}\mathrm{(NN)_3^{3+}} \quad (18)$$

For reaction between O_2 and $(^2E)\mathrm{Cr(NN)_3^{3+}}$, k_q values are 2–3 orders of magnitude smaller than the diffusion-controlled limit. Inasmuch as the two lowest excited states of O_2 occur at $\sim 12.9 \times 10^3\ \mathrm{cm^{-1}}$ ($^1\Sigma_g^+$) and $\sim 7.9 \times 10^3\ \mathrm{cm^{-1}}$ ($^1\Delta_g$) (*37*) and the energy of $(^2E)\mathrm{Cr(NN)_3^{3+}}$ is $\sim 13.7 \times 10^3\ \mathrm{cm^{-1}}$, energy transfer to form $^1O_2$ (reaction (19)) is energetically possible and spin-allowed; quenching via electron transfer does not appear consequential (*6*, *27*).

$$(^2E)\mathrm{Cr(NN)_3^{3+}} + {}^3O_2 \rightarrow (^4A_2)\mathrm{Cr(NN)_3^{3+}} + {}^1O_2 \quad (19)$$

Photoaquation of $(^2T_1/{}^2E)\mathrm{Cr(NN)_3^{3+}}$ Complexes

Quantum Yields

Continuous photolysis of $\mathrm{Cr(NN)_3^{3+}}$ in neutral or basic aqueous solutions leads to substitution of one polypyridyl ligand by two water (or hydroxy) molecules (*8*, *10*, *17*). The spectral changes and formation of free polypyridine mimic those observed for the corresponding thermal reactions (*7*, *10*). For $\mathrm{Cr(bpy)_3^{3+}}$ at pH 9.6, the absorption spectral changes of continuously photolyzed (*8*), repeatedly flashed (*8*), and thermally aquated solutions (*7*) are identical, with isosbestic points at 306, 270, 262, and 254 nm (*8*). The overall stoichiometry of the photoaquation (reaction (20)) is similar to reaction (1), where Φ_{rx} is the observed quantum yield for NN release.

$$\mathrm{Cr(NN)_3^{3+}} \xrightarrow{h\nu} {}^*\mathrm{Cr(NN)_3^{3+}} \xrightarrow[\mathrm{OH^-/H_2O}]{\Phi_{rx}} \mathrm{Cr(NN)_2(OH)_2^+} + \mathrm{NN} \quad (20)$$

The complexes are relatively inert toward thermal- (*7*, *10*) and photosolvolysis (*8*, *21*) in acidic media. This observation, together with the observation that k_{th} of reaction (1) and Φ_{rx} of the photoreaction (20) show very similar pH dependences, (Fig. 3) suggests that the two reactions proceed through a common ground state intermediate. The interchange mechanism alluded to before applies equally to reaction (20), where the intermediate species is formed by attack of H_2O on the $^*\mathrm{Cr(NN)_3^{3+}}$ metal core (*8*, *17*). Flash photolysis experiments on $\mathrm{Cr(bpy)_3^{3+}}$ in acidic media reveal transient bleaching of the ground state following decay of the $^2T_1/{}^2E$ states implying formation of a nonabsorbing (at the monitoring wavelength) intermediate. Recovery of ground state absorption proceeds via acid-dependent and -independent paths believed to be the equivalent of reaction (2) with rate constants of $4 \times 10^5\ \mathrm{M^{-1}s^{-1}}$ and $\leq 10\ \mathrm{s^{-1}}$ (*8*), respectively. The H^+-dependent path is believed (*38*) to be the primary reaction leading to the relative photochemical and thermal stability of $\mathrm{Cr(bpy)_3^{3+}}$ in acid solution. However, because of the ground state quenching phenomenon, measurements of Φ_{rx} and $^2\tau_{obs}$ must be made in well defined solution media. These data are summarized in Table 3 for 12 $\mathrm{Cr(NN)_3^{3+}}$ complexes.

Table 3. Photochemical and Photophysical Characteristics of $\mathrm{Cr(NN)_3^{3+}}$ at 22°C in Deaerated Solutions [a]

NN	[Cr(III)] (mM)	Φ_{rx}(pH)	$^2\tau_{obs}$, ms	$^2k_{rx}$, $\mathrm{s^{-1}}$
bpy	1.0	0.13(9.3)	0.071	1.6×10^3
4,4′-Me_2bpy	0.12	0.002(5.1)		
		0.06(9–10.5)	0.18	3.5×10^2
4,4′-Ph_2bpy	0.048	0.011(5.1)		
		0.02(9–10.5)	0.050	4.2×10^2
5-Clphen	0.14	0.002(5.1)		
		0.011(9–10.5)	0.086	1.3×10^2
5-Brphen	0.12	0.006(5.1)		
		0.008(9–10.5)	0.063	1.3×10^2
phen	1.5	0.0005(5.1)		
		0.006(9–10.5)	0.074	7.5×10^1
5-Mephen	0.12	0.004(5.1)		
		0.012(9–10.5)	0.18	6.7×10^1
5,6-Me_2phen	0.11	0.005(5.1)		
		0.007(9–10.5)	0.19	3.4×10^1
4,7-Me_2phen	0.11	0.0003(5.1)		
		0.004(9–10.5)	0.25	1.4×10^1
3,4,7,8-Me_4phen	0.084	0.0002(5.1)		
		0.002(9–10.5)	0.21	7.6
5-Phphen	0.072	0.003(5.1)		
		0.006(9–10.5)	0.081	7.4×10^1
4,7-Ph_2phen	0.034	0.0012(5.1)		
		0.0014(9–10.5)	0.074	1.9×10^1

[a] See reference (*21*) for experimental conditions.

The population of $^2T_1/{}^2E$ depends on the efficiency of intersystem crossing ($^4\eta_{isc}$) from $^4T_2$ to $^2T_1/{}^2E$ where $^4\eta_{isc} = {}^4k_{isc}/({}^4k_{isc} + {}^4k_{nr} + {}^4k_{rx})$. The value of Φ_{rx} for each complex is a result of all the processes that eventually lead to the aquated products. As can be seen in Table 3, all the observed values of Φ_{rx} reach a plateau in the vicinity of pH 9–10 and decrease as the solution is made more acidic. If it is true, as is believed, that all $^2T_1/{}^2E$ species that pass to $\mathrm{Cr(NN)_3(OH)^{2+}}$ in alkaline solution lead rapidly, irreversibly, and quantitatively to $\mathrm{Cr(NN)_2(OH)_2^+}$, then $\Phi_{rx} \simeq ({}^4\eta_{isc}{}^2\eta_{rx}) + {}^4\eta_{rx}$ where $^2\eta_{rx}$ is the efficiency of reaction out of $^2T_1/{}^2E$ ($= {}^2k_{rx}^2\tau_{obs}$) and $^4\eta_{rx}$ is the efficiency of reaction out of $^4T_2$. Inasmuch as the portion of the observed value of Φ_{rx} that cannot be quenched by I^-, a very efficient doublet state quencher, is <10% of Φ_{rx} (*15*), $^4\eta_{rx}$ may be neglected. Therefore, $\Phi_{rx} \simeq {}^4\eta_{isc}{}^2k_{rx}{}^2\tau_{obs}$. Taking $^4\eta_{isc} \sim 1$ (*39*), $\Phi_{rx} = {}^2k_{rx}{}^2\tau_{obs}$. Calculated values of $^2k_{rx}$ are collected also in Table 3.

Ligand Substituent Effect

According to our model, $^2k_{rx}$ reflects the ease with which the $\mathrm{Cr(NN)_3(H_2O)^{3+}}$ intermediate forms upon interaction of the solvent with $(^2T_1/{}^2E)\mathrm{Cr(NN)_3^{3+}}$. It is possible to visualize the distortion and loosening of the ligand structure in order to accomodate the incoming water molecule; the intermediate may be seven-coordinate in nature with some capped octahedral or pentagonal bipyramidal structure (*40*).[2] Thus, the flexibility of the ligand structure and the extent of hydrophilicity in the vicinity of the interligand pockets will dictate the value of $^2k_{rx}$. Examination of the data of Table 3 shows that the more flexible bpy framework is more amenable to distortion than is the more rigid phen framework; in all cases, $^2k_{rx}$ for bpy complexes is larger than for phen. The highly

[2] It is worth noting that seven-coordinate geometry for the first row transition metals is no longer an unusual geometry. See, for example, the extensive review by Drew (*41*).

electronegative chlorine and bromine atoms in the 5-position of phen clearly facilitate water entry (compared to unsubstituted phen) into the pockets thereby providing an increased hydrophilic environment. Methyl and phenyl derivatives, especially multiply substituted, exhibit lower values of $^2k_{rx}$ due to decreased hydrophilic environment. The values of $^2k_{rx}$, therefore, reflect the competition between the hydrophilic quality of the interligand pockets and the flexibility of the ligands in order to accomodate distortion.

Solution Medium Effects

One of the most interesting aspects of the photochemical studies of $Cr(NN)_3^{3+}$ complexes is the alteration of the solution medium and its effect on the properties of the excited state complexes. One such effect, pH changes on Φ_{rx}, has already been noted.

Ground state quenching of $^2T_1/^2E$ results in a diminution in the population of the states and must consequently result in a decrease of the quantum yields of the various processes that arise from doublet states. Φ_{rx}, for example, is expected to decrease with increased [substrate] in 1.0 *M* NaCl inasmuch as $\Phi_{rx} = {}^2k_{rx}{}^2\tau_{obs}$ and $^2\tau_{obs} = 1/(^2k_0 + {}^2k_g[\text{substrate}])$. Although Φ_{rx} has been determined for most of the $Cr(NN)_3^{3+}$ complexes over a concentration in substrate of greater than one order of magnitude (*21*), only three complexes (NN = 5-Brphen, 5-Phphen, and 4,7-Ph_2phen) show the effect outside of experimental error. This limitation arises from the very low values of Φ_{rx} (Table 3). This notwithstanding, the resulting ^2k_g values obtained from Φ_{rx} studies agree reasonably well with ^2k_g values obtained from $^2\tau_{obs}$ studies in 1.0 *M* media (*21*).

Doublet state quenchers such as I^- and O_2 act to decrease the population of ^2E and the value of Φ_{rx}. Thus, with increasing concentration of I^-, Φ_{rx} diminishes to a plateau at $[I^-] \sim 0.1$–0.4 *M* in deaerated alkaline solution for both $Cr(bpy)_3^{3+}$ and $Cr(phen)_3^{3+}$; at that $[I^-]$, ~99.99% of the reaction from $^2T_1/^2E$ is quenched. The observed value of Φ_{rx} is 2×10^{-3} and 7×10^{-4} for $Cr(bpy)_3^{3+}$ and $Cr(phen)_3^{3+}$, respectively, at pH 9.3 (*15*). The lower value of Φ_{rx} for the phen complex is attributed to the $^4T_2$ state of this complex accomodating less distortion than the bpy complex owing to the greater rigidity of the phen framework. The effect of the presence of air is to reduce Φ_{rx} from a value of 0.13 for $Cr(bpy)_3^{3+}$ in alkaline solution (absence of I^-) to a value of 0.10 in air-saturated solution.

The value of Φ_{rx} for the photoaquation of $Cr(bpy)_3^{3+}$ in O_2-free alkaline solution increases from 0.089 at 279.5 K to 0.13 at 309.5 K(*15*). Activation parameters are $\Delta H_{rx}^{\ddagger} = 9.7$ kcal mol^{-1} and $\Delta S_{rx}^{\ddagger} = -11$ cal $deg^{-1}mol^{-1}$. Thus, the enthalpy of activation for reaction from $^2T_1/^2E$ is considerably less, by ~13 kcal mol^{-1}, than the comparable reaction from the $^4A_2$ ground state, but the entropy of activation is about the same; the photoreaction is faster by about ten orders of magnitude. Inasmuch as $^2T_1/^2E$ and $^4A_2$ have the same geometry, the greater excited state photoreaction is attributed to the $^2T_1$ state which we suggest possesses some degree of reduced electron density in the t_{2g} levels compared to the ^2E state; this aspect would result in less reorganizational energy being required to form the activated complex (*42*).

Table 4. Summary of the General Mechanism for the Photochemistry and Photophysics of $Cr(NN)_3^{3+}$ Complexes in Aqueous Solution

Reaction	Mechanism
$(^4A_2)Cr(NN)_3^{3+} \xrightarrow[I_a]{h\nu} (^4T_2, a^4T_1, b^4T_1)Cr(NN)_3^{3+}$	Light absorption
$(^4T_2, a^4T_1, b^4T_1)Cr(NN)_3^{3+} \rightarrow (^4T_2)Cr(NN)_3^{3+}$	Internal conversion
$(^4T_2)Cr(NN)_3^{3+} \xrightarrow{^4k_{nr}} (^4A_2)Cr(NN)_3^{3+}$	Nonradiative decay
$\xrightarrow{^4k_{isc}} (^2T_1/^2E)Cr(NN)_3^{3+}$	Intersystem crossing
$\xrightarrow{^4k_{rx},H_2O} Cr(NN)_3(H_2O)^{3+}$	Chemical reaction
$(^2T_1/^2E)Cr(NN)_3^{3+} \xrightarrow{^2k_{nr}} (^4A_2)Cr(NN)_3^{3+}$	Nonradiative decay
$\xrightarrow{^2k_{rad}} (^4A_2)Cr(NN)_3^{3+} + h\nu'$	Phosphorescence
$\xrightarrow{^2k_{rx},H_2O} Cr(NN)_3(H_2O)^{3+}$	Chemical reaction
$\Downarrow H^+$	
$\xrightarrow{^2k_{rx},OH^-} Cr(NN)_3(OH)^{2+}$	Chemical reaction
$(^2T_1/^2E)Cr(NN)_3^{3+} + (^4A_2)Cr(NN)_3^{3+} \xrightarrow{^2k_g,Cl^-} 2(^4A_2)Cr(NN)_3^{3+}$	Ground state quenching
$Cr(NN)_3(H_2O)^{3+} \rightleftharpoons (^4A_2)Cr(NN)_3^{3+} + H_2O$	Acid-independent decay of intermediate
$\xrightarrow{H^+} (^4A_2)Cr(NN)_3^{3+} + H_2O$	Acid-dependent decay of intermediate
$\xrightarrow[H_2O]{H^+} Cr(NN)_2(H_2O)_2^{3+} + NNH^+$	Labilization of intermediate
$Cr(NN)_3(OH)^{2+} \xrightarrow{OH^-} Cr(NN)_2(OH)_2^+ + NN$	Labilization of deprotonated intermediate

Summary

From the various studies, a general mechanism has evolved for the photochemistry and photophysics of $Cr(NN)_3^{3+}$ complexes in aqueous solutions which is summarized in Table 4.

Unaswered Questions and Future Directions

As in all areas of research, the more one knows, the more questions are raised. Despite the enormous body of knowledge on the photochemistry and photophysics of Cr(III) complexes in general, and $Cr(NN)_3^{3+}$ in particular, there remain many unanswered questions that will serve as the basis for future research.

1) What is the energy of the *thexi* $^4T_2^0$ state, its geometry, and its lifetime? Without any detectable fluorescence from that state, it will remain an enigma. Perhaps it can be detected by its absorption spectrum using picosecond pulsed laser excitation.

2) What is the origin of the wavelength dependence of the quenchable and unquenchable photoaquation quantum yields and the phosphorescence quantum yield (*43*, *44*) which shows a sharp decrease between 470 and 510 nm? It is clear that $^4\eta_{isc}$ is wavelength-dependent in that region (*45*) suggesting that prompt intersystem crossing and photoreaction occur at an energy higher than that of the *thexi* $^4T_2^0$ state (*46*).

3) What is the mechanism by which solution medium affects the value of $^2\tau_{obs}$ and Φ_{rx}? We know that the addition of ClO_4^- to aqueous solutions of $Cr(bpy)_3^{3+}$prolongs the lifetime but decreases the quantum yield of photoaquation (*47*). We also know that DMF (*25*), CH_3CN and mixed CH_3CN-H_2O (*48*) decrease both $^2\tau_{obs}$ (*25*, *48*) and Φ_{rx} (*17*, *48*). Details for other nonaqueous solvents and mixed solvents are not available.

4) To what extent can $Cr(NN)_3^{3+}$ complexes be used in solar energy conversion and storage schemes? We have addressed the question of the potentiality of these complexes (*49*) and find that their photochemical and thermal stabilities in acidic solution, their long-lived excited states, and their excited state redox potentials are positive aspects; their absorption spectra and lability of their corresponding Cr(II) species are negative aspects.

Acknowledgment

We are particularly grateful to our associates, Drs. Marian S. Henry, R. Sriram, and Mary Jamieson, without whose efforts much of our work would not have been realized. We are grateful also for the support we have obtained through the years from the Natural Sciences and Engineering Research Council of Canada, the Fonds F.C.A.C. du Quebec, the National Science Foundation, and the North Atlantic Treaty Organization.

Literature Cited

(1) For an earlier review, see: Zinato, E., in "Concepts of Inorganic Photochemistry," Adamson, A. W., and Fleischauer, P. D. (*Editors*), Wiley, New York, **1975**, ch. 4.
(2) Forster, L. S., *Adv. Chem. Ser.*, **150**, 172 (1976); Fleischauer, P. D., Adamson, A. W., and Sartori, G., *Prog. Inorg. Chem.*, **17**, 1 (1972).
(3) Kirk, A. D., J. CHEM. EDUC., **60**, 843 (1983).
(4) Jamieson, M. A., Serpone, N., and Hoffman, M. Z., *Coord. Chem. Rev.*, **39**, 121 (1981).
(5) König, E., and Herzog, S., *J. Inorg. Nucl. Chem.*, **32**, 585 (1970).
(6) Serpone, N., Jamieson, M. A., Henry, M. S., Hoffman, M. Z., Bolletta, F., and Maestri, M., *J. Amer. Chem. Soc.*, **101**, 2907 (1979).
(7) Maestri, M., Bolletta, F., Serpone, N., Moggi, L., and Balzani, V., *Inorg. Chem.*, **15**, 2048 (1976).
(8) Maestri, M., Bolletta, F., Moggi, L., Balzani, V., Henry, M. S., and Hoffman, M. Z., *J. Amer. Chem. Soc.*, **100**, 2694 (1978).
(9) Jamieson, M. A., Serpone, N., and Maestri, M., *Inorg. Chem.*, **17**, 2432 (1978).
(10) Maestri, M., Bolletta, F., Moggi, L., Jamieson, M. A., Serpone, N., Henry, M. S., and Hoffman, M. Z., *Inorg. Chem.*, **22**, 2503 (1983).
(11) Fleischauer, P. D., Adamson, A. W., and Sartori, G., *Prog. Inorg. Chem.*, **17**, 1 (1972).
(12) Balzani, V., and Carassiti, V., "Photochemistry of Coordination Compounds," Academic Press, New York, **1970.**
(13) Ballardini, R., Varani, G., Scandola, F., and Balzani, V., *J. Amer. Chem. Soc.*, **98**, 7432 (1976).
(14) Kane-Maguire, N. A. P., Conway, J., and Langford, C. H., *J. Chem. Soc., Chem. Commun.*, 801 (1974).
(15) Jamieson, M. A., Serpone, N., and Hoffman, M. Z., *J. Amer. Chem. Soc.*, **105**, 2933 (1983).
(16) Kirk, A. D., and Porter, G. B., *J. Phys. Chem.*, **84**, 887 (1980).
(17) Henry, M. S., and Hoffman, M. Z., *Adv. Chem. Ser.*, **168**, 91 (1978).
(18) Gutierrez, A. R., and Adamson, A. W., *J. Phys. Chem.*, **82**, 902 (1978).
(19) Indelli, M. T., Ballardini, R., Bignozzi, C. A., and Scandola, F., *J. Phys. Chem.*, **86**, 4284 (1982).
(20) Henry, M. S., *J. Amer. Chem. Soc.*, **99**, 6138 (1977).
(21) Serpone, N., Jamieson, M. A., Sriram, R., and Hoffman, M. Z., *Inorg. Chem.*, **20**, 3983 (1981).
(22) Sriram, R., Hoffman, M. Z., Jamieson, M. A., and Serpone, N., *J. Amer. Chem. Soc.*, **102**, 1754 (1980).
(23) Kirk, A. D., *Theor. Chim. Acta*, **20**, 113 (1971); Jezowska-Trzebiatowska, B., and Dominiak-Dzik, G., *J. Mol. Struct.*, **46**, 339 (1978).
(24) Jamieson, M. A., Serpone, N., Hoffman, M. Z., and Bolletta, F., *Inorg. Chim. Acta*, **72**, 247 (1983).
(25) Van Houten, J., and Porter, G. B., *Inorg. Chem.*, **18**, 2053 (1978).
(26) Serpone, N., Jamieson, M. A., Emmi, S., Fuochi, P. G., Mulazzani, Q. G., and Hoffman, M. Z., *J. Amer. Chem. Soc.*, **103**, 1091 (1981).
(27) Brunschwig, B., and Sutin, N., *J. Amer. Chem. Soc.*, **100**, 7568 (1978).
(28) Sutin, N., *in* "Tunnelling in Biological Systems," Chance, B. (*Editor*), Academic Press, New York, **1979**; Sagi, T., and Aoyagui, S., *Electroanal. Chem. Interfac. Electrochem.*, **60**, 1 (1975); Baker, B. R., and Mehta, B. D., *Inorg. Chem.*, **4**, 848 (1965); Hughes, M. C., and Macero, D. J., *Inorg. Chem.*, **13**, 2739 (1974).
(29) Ballardini, R., Varani, G., Indelli, M. T., Scandola, F., and Balzani, V., *J. Amer. Chem. Soc.*, **100**, 7219 (1978).
(30) Lin, C. T., Bottcher, W., Chou, M., Creutz, C., and Sutin, N., *J. Amer. Chem. Soc.*, **98**, 6536 (1976).
(31) Sargeson, A. M., and Buckingham, D. A., "Chelating Agents and Metal Chelates," Dwyer, F. P., and Mellor, D. P. (*Editors*), Academic Press, New York, **1964**, p. 269.
(32) Bolletta, F., Maestri, M., Moggi, L., and Balzani, V., *J. Chem. Soc., Chem. Commun.*, 901 (1975).
(33) Juris, A., Manfrin, M. F., Maestri, M., and Serpone, N., *Inorg. Chem.*, **17**, 2258 (1978).
(34) Marcus, R. A., *J. Chem. Phys.*, **24**, 966 (1956); Marcus, R. A., *Ann. Rev. Phys. Chem.*, **15**, 155 (1964); Marcus, R. A., *J. Phys. Chem.*, **43**, 679 (1965); Marcus, R. A., *J. Phys. Chem.*, **43**, 2654 (1965).
(35) Rehm, D., and Weller, A., *Ber. Bunsenges. Phys. Chem.*, **73**, 834 (1969); Rehm, D., and Weller A., *Israel J. Chem.*, **8**, 259 (1970).
(36) Jorgensen, C. K., "Absorption Spectra and Chemical Bonding in Complexes," Pergamon Press, Oxford, **1962.**
(37) Herzberg, G., "Spectra of Diatomic Molecules," Van Nostrand, Princeton, NJ, **1950.**
(38) Sriram, R., Henry, M. S., and Hoffman, M. Z., *Inorg. Chem.*, **18**, 1727 (1979).
(39) Serpone, N., Jamieson, M. A., and Hoffman, M. Z., *J. Chem. Soc., Chem. Commun.*, 1006 (1980).
(40) Hoffmann, R., Beier, B. F., Muetterties, E. L., and Rossi, A. R., *Inorg. Chem.*, **16**, 511 (1977).
(41) Drew, M. G. B., *Prog. Inorg. Chem.*, **23**, 67 (1977), and references therein.
(42) Jamieson, M. A., Serpone, N., Henry, M. S., and Hoffman, M. Z., *Inorg. Chem.*, **18**, 214 (1979).
(43) Langford, C. H., and Sasseville, R. L. P., *Inorg. Chem.*, **19**, 2850 (1980).
(44) Jamieson, M. A., Ph.D. Dissertation, Concordia University, Montreal, Canada, **1983.**
(45) Sasseville, R. L. P., and Langford, C. H., *J. Amer. Chem. Soc.*, **101**, 5834 (1979).
(46) Serpone, N., 5th Microsymposium on the Photochemistry and Photophysics of Coordination Compounds, Gif-sur-Yvette, France, August 1–5, **1982**, Abstract A8.
(47) Sriram, R., and Hoffman, M. Z., 5th Microsymposium on the Photochemistry and Photophysics of Coordination Compounds, Gif-sur-Yvette, France, August 1–5, **1982**, Abstract A23.
(48) Jamieson, M. A., Langford, C. H., Serpone, N., and Hersey, M. W., *J. Phys. Chem.*, **87**, 1004 (1983).
(49) Hoffman, M. Z., and Serpone, N., *Israel J. Chem.*, **22**, 91 (1982).